Mine Water and the Environment (2019) 38:528–535
https://doi.org/10.1007/s10230-019-00616-2

TECHNICAL ARTICLE

Multi-field Coupling of Water Inrush Channel Formation in a Deep Mine with a Buried Fault

Wenbin Sun[1] · Yanchao Xue[1,2] · Tingting Li[1] · Weitao Liu[1]

Received: 19 November 2017 / Accepted: 15 July 2019 / Published online: 19 July 2019

Abstract
Due to the high pressure of confined water in deep mines, the incidence of water inrush disasters in China caused by geological structures, especially faults, are becoming more frequent and more complicated. Using the Comsol numerical simulation software, we analyzed the formation and evolution of a water inrush channel in the floor of a deep mine with buried faults. The numerical model was set up using geological data from an actual coal mine that is highly threatened by confined water with buried faults. The results show that the stress became more and more concentrated near the buried fault as the working face advanced. The flow velocity inside the fault was much greater than in the floor, which means that the buried structure was important in the ascension of the confined water and destruction of the floor. A water inrush channel formed when the failure zone connected with the fissures of the buried fault.

Keywords Buried structure · Fault activation · Activation of water inrush · Numerical simulation

Introduction

The geological structure of the strata surrounding deep mines can be complex (Wang et al. 2017; Yin et al. 2018a, b; Zhang et al. 2018), which increases the probability of water inrush. Water inrush disasters have frequently occurred in China's coal mines during the past 20 years, making them the second highest cause of accidental deaths, and producing numerous casualties and tremendous economic loss (Li et al. 2015). Buried fault structures account for up to 79.5% of such disasters (Sun et al. 2019; Shao et al. 2019; Xiong and Wang 2014; Zhou et al. 2018).

The critical empirical parameter to prejudge the risk of water inrush disaster is the water inrush coefficient, which is defined as the ratio between the water pressure and the thickness of the aquifuge. This coefficient was proposed in the 1960s and is widely used in China. Several modifications have been investigated to better reflect actual conditions (Li et al. 2015, 2018). Feng et al. (2009) introduced the concept of water-resistant key strata to build a mechanical model. Zhang (2004) applied elastoplastic theory and mathematical statistics to analyze the water inrush mechanism in an intact and fractured floor, and studied the dynamic mechanism of floor water inrush in detail. Grasemann et al. (2011), Wang et al. (2014) and Zhou et al. (2018) studied a fault-induced water inrush from different angles and analyzed the characteristics of the stress evolution, as well as the formation mechanism of a water inrush channel due to fault flexible shear by means of RFPA, FLAC-3D, experimental simulation, etc. Lu and Wang (2015) divided the fracturing evolution of a fault into three stages, i.e. a quiet period, an active period, and the eventual eruptive period. The lagging mechanism of water inrush through the mine floor with a buried fault and a confined aquifer was revealed in experimental and numerical simulations by Zhang et al. (2017).

Risk evaluation has also been investigated, and corresponding geological assessment models (Dumpleton et al. 2001; Bukowski 2011; Sun and Xue 2018) and mathematical models (Hodlur et al. 2002; Wang et al. 2012; Wu et al. 2017) are established. However, the mechanism and characteristics of inrush channel formation under the condition of multi-fields coupling are not yet clear (Bereslavskii 2011; Odintsev and Miletenko 2015). Therefore, we felt there was a need for an in-depth study, to mitigate such hazards during future mining.

✉ Wenbin Sun
swb@sdust.edu.cn

[1] College of Mining and Safety Engineering, Shandong University of Science and Technology, Qingdao 266590, China

[2] School of Resources and Civil Engineering, Northeastern University, Shenyang 110819, China

Geological Structure and Study Site

Engineering Background

The studied mine is located in Jining city, Shandong province, east of China, covering an area of ≈20.8 km^2. The mine is a structural basin, though its shape is incomplete due to fault cutting. Strata inclination is shallower in the west and steeper in the east. There faults in the area are mainly north–south. There are 44 faults with fall heights greater than or equal to 20 m in the mine, and the structure type is moderately complex (Fig. 1). There are few northwest faults, and the fall and extent of northwest faults is small and short.

Due to the north–south, near earth–west, and northeast faults, the mine basically consists of several stratigraphic blocks, as shown by the differently colored areas in Fig. 1. Many blocks of the lower coal seams directly interface with the Ordovician limestone, posing a great threat to coal production. The tensile normal faults with large falls can also lead the confined karst water to the excavated area. In particular, after large areas are mined, the ground stress is concentrated on the coal pillars, so that the buried faults may be activated to become water-conducting faults. Therefore, the faults make the hydrogeological conditions more complex.

Study Site

The lower coal group mainly consists of coal seams 16 and 17, and the main underlying aquifer is an Ordovician limestone formation. The no. 1 coal face, the first face of coal seam 17, is located in the west wing of the mine and is being mined by longwall methods. The composite strata column, according to drilling data from the no. 1 working face, is shown as Fig. 2. The thickness of the coal seam ranges from 3 to 7 m. The depth of the no. 1 working face ranges from 1280 to 1320 m, and its dip angle ranges from 0° to 5°.

The north–south buried faults are more developed in this area, and multiple faults have reduced the distance between the no. 17 coal and the Ordovician limestone. The underlying aquifuge is located 38-50 m below the no. 17 coal seam and above the Ordovician limestone. It is mainly composed of mudstone, siltstone, fine sandstone, and limestone. In areas where the aquifuge is relatively thin and where faults are located, its water resistance will

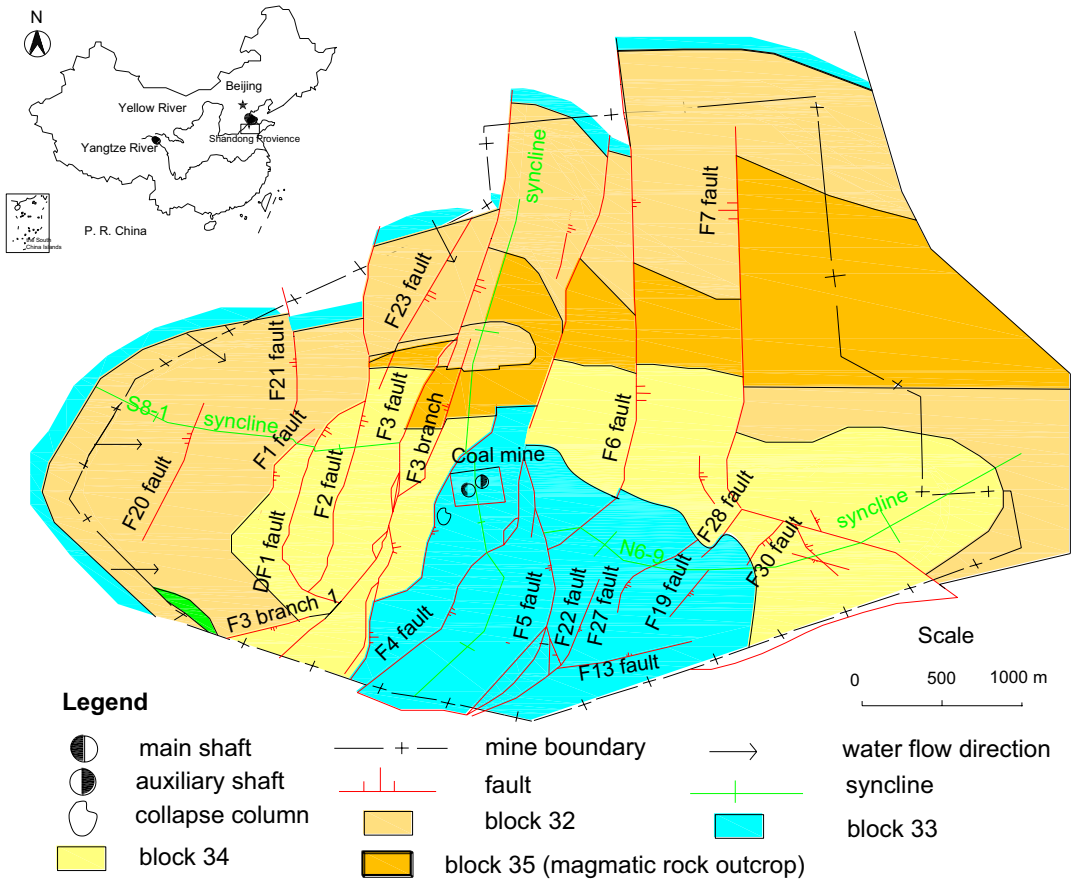

Fig. 1 Schematic diagram of mine tectonics

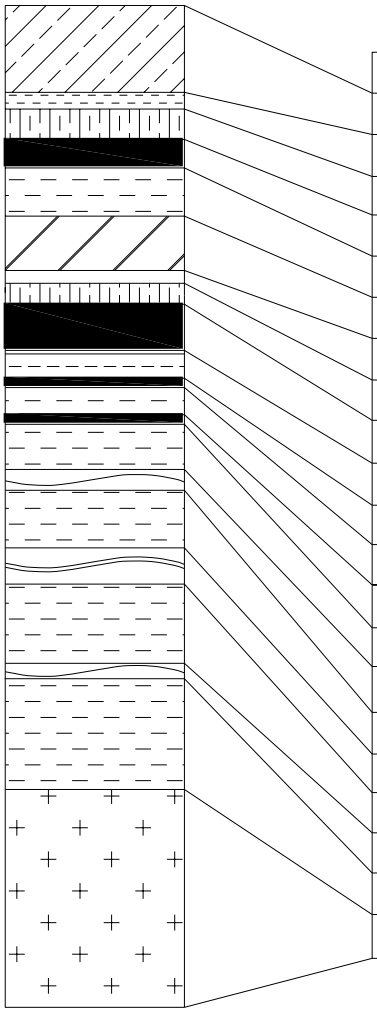

Rock thickness(m)	Depth(m)	Lithology
18.62	1273.08	
0.51	1273.59	Mudstone
2.89	1276.48	Eleventh limestone
1.60	1278.08	Coal seam 16
3.47	1281.55	Mudstone
3.90	1285.45	Fine sandstone
0.92	1286.37	Mudstone
3.95	1290.32	Limestone
5.00	1295.32	**Coal seam 17**
3.48	1296.31	Mudstone
0.38	1296.69	Coal seam 18_{up}
3.40	1300.09	Mudstone
0.45	1300.54	Coal seam 18_{down}
5.07	1305.61	Mudstone
1.20	1306.81	Twelfth limestone
6.76	1313.57	Mudstone
4.35	1317.92	Thirteenth limestone
9.37	1327.29	Mudstone
0.37	1327.66	Fifteenth limestone
14.76	1342.42	Mudstone
70.00	1412.42	Ordovician limestone

Fig. 2 Composite strata column of no. 1 working face in the mine

be greatly deteriorated. There is a normal fault X1 near the working face with a dip angle of 70° and a height of 30 m (Fig. 3). Exploration boreholes drilled before the no. 17 coal was exploited revealed that this fault was filled with fault breccia and fault gouge, and did not contain water, indicating that the fault was likely water resistant. However, the fault could potentially be gradually activated, hydraulically connecting the aquifer with the mined area as excavation develops.

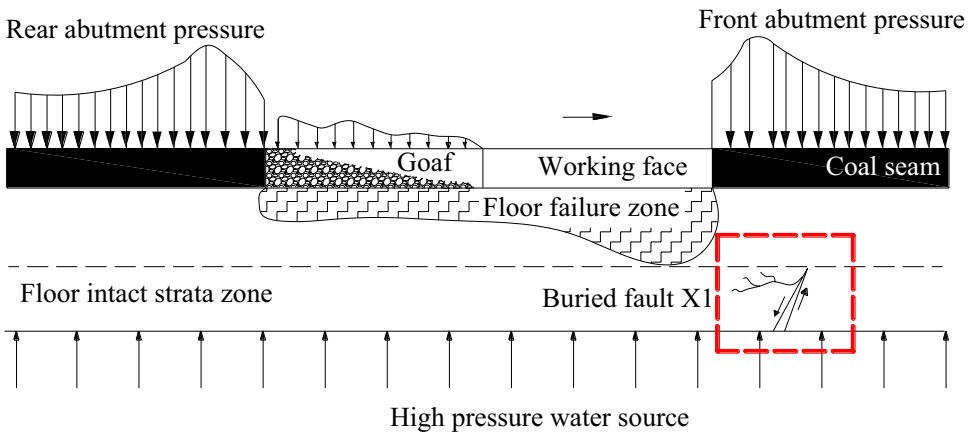

Fig. 3 Schematic diagram of floor water inrush in no. 1 working face

Water Inrush Channel Formation Mechanism

As shown in Fig. 3, the existence of the fault greatly reduced the water resistance of the floor strata, as the fault was transformed into a potential water inrush channel. On the one hand, the stress field caused by the combination of mining, ground pressure, and hydraulic pressure affects the fracture structure, displacing the floor and activating the fault, which leads to confined water head intrusion and accelerates the characteristic change of the seepage field of the confined water. On the other hand, tectonic stress is generated around the fractured geological structure, further damaging the floor and increasing fracturing. According to the minimum path principle, the fissures will develop to the floor failure zone, and change the position of the inrush channel.

Numerical Simulation

Comsol multiphysics is a professional finite element numerical analysis software package with an interactive system for calculations and simulations based on a multiphysical model of partial differential equations. The advantages of this software lie in its multi-physical coupling: the Forchheimer nonlinear flow equation is coupled with the Darcy linear flow equation and the free flow *N*–*S* equation. Comsol takes the continuity of flow as the basic equation and meets the same water pressure and equal flow rate at the interfaces of aquifer-fault, fault-cracked rock, cracked rock-roadway, etc. to solve the fault water inrush problem.

A simple two-dimensional numerical model that contains a buried fault was established based on the no. 17 coal seam at the mine (Fig. 4). The size of the model was 160 m (length) × 55 m (width), and the mesh was divided into 8800 units. The working direction of the working face was taken as the *X*-axis and the direction of gravity was the *Y*-axis to facilitate the analysis of water inrush through the buried fault. From top to bottom, the strata were divided into four strata, namely, the overlying strata, the coal seam, the floor aquifuge, and the floor aquifer, with thickness of 5, 5, 40, and 5 m, respectively. The physical and mechanical parameters of the strata are listed in Table 1. The mining depth is 1300 m (below the surface) and the hydraulic pressure of the confined water is 6 MPa. The buried fault structure, with a dip angle of 70° and a height of 30 m, which is filled with soft-rheology-plastic fault gouge and siltstone, is viewed as a weak zone. The rock strata and fault were assumed to be homogeneous and isotropic during the finite element analysis.

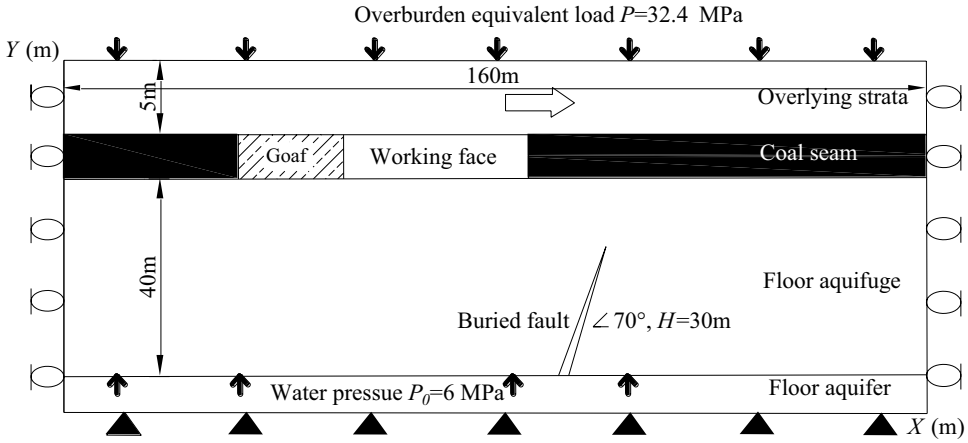

Fig. 4 Numerical calculation model

Table 1 Rock mechanics parameters

Rock name	Thickness (m)	Tensile strength (MPa)	Elastic modulus (10^3 MPa)	Poisson ratio	Cohesive force (MPa)	Friction angle (°)	Permeability (m^2)	Bulk density (10^3 kg/m^3)
Overlying strata	5	3.0	23	0.25	5.0	20	1.3×10^{-7}	1.8
Coal seam	5	1.5	5	0.25	2.1	15	4.2×10^{-6}	1.3
Aquifuge	40	5.4	45	0.18	5.8	46	1.3×10^{-7}	2.25
Aquifer	5	4.1	15	0.28	3.5	41	–	2.1
Fault	–	0.3	4	0.3	0.01	10	2.6×10^{-6}	2.3

Boundary Conditions

The design depth of the coal seam was 1300 m with an average bulk density of the overlying strata of 25 kN/m^3. A uniform load of 32.4 MPa was applied to simulate the overlying strata thickness of 1295 m; the weight was defined using the software. The lower end of the model was fixed and the left and right sides were supported by rollers. Mohr–Coulomb yield criterion was adopted in the simulation. For the fluid flow analysis, the model simulated pore water pressure flow, with an aquifer water pressure of 6 MPa; an atmospheric pressure of 0 was applied as a boundary condition at the working face. Other boundaries were set to no outflow and inflow.

Mining Scheme Design

In the model, the coal seam was mined for 20 m along the x-axis in each step and the total advancing distance was 120 m. The calculating procedures follows:

1. With different advancing distances, the mechanism of inrush channel formation can be easily deduced by comparing the variations in stress and water velocity inside and near the fault. The effect of the fault on the hydraulic conductivity of the confined water can be seen in Figs. 5 and 6.
2. By analyzing the floor failure depth, the area consisting of damage zones that directly connect the mining goaf and fault can be seen as water-conducting fractured zones, as shown in Fig. 7.

Results and Discussions

Analysis of Water Inrush Channel Formation Mechanism in Floor with Buried Faults

Stress Field Variation Analysis

After the coal seam was mined, the original stress balance was destroyed, and the stress was concentrated in the surrounding rock. Stress was unloaded near the mining goaf, especially at both ends of the working face and open-off cut, showing a symmetrical "ellipse-shape", as found by Zhou et al. (2018). As the working face advanced, a 3 m wide stress-concentrated area appeared in the floor rock strata above the buried fault and below the working face; the maximum stress was 167 MPa. At this time, the stress concentration in the middle and upper part of the buried fault exceeded that in the floor; the stress near the fault zone was 67 MPa. This is because the fault zone hindered the transfer of secondary stress caused by the mining, concentrating the surrounding rock stress in the excavation area and fault zone.

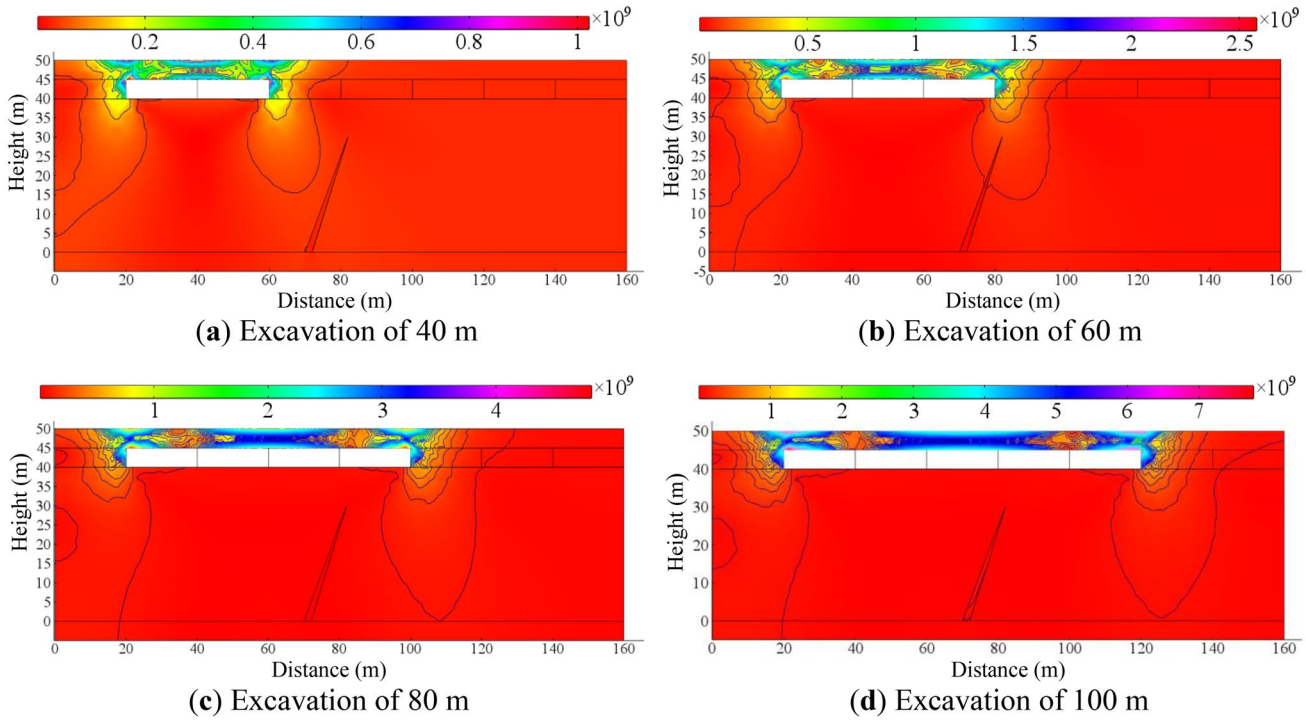

Fig. 5 Stress-field nephogram

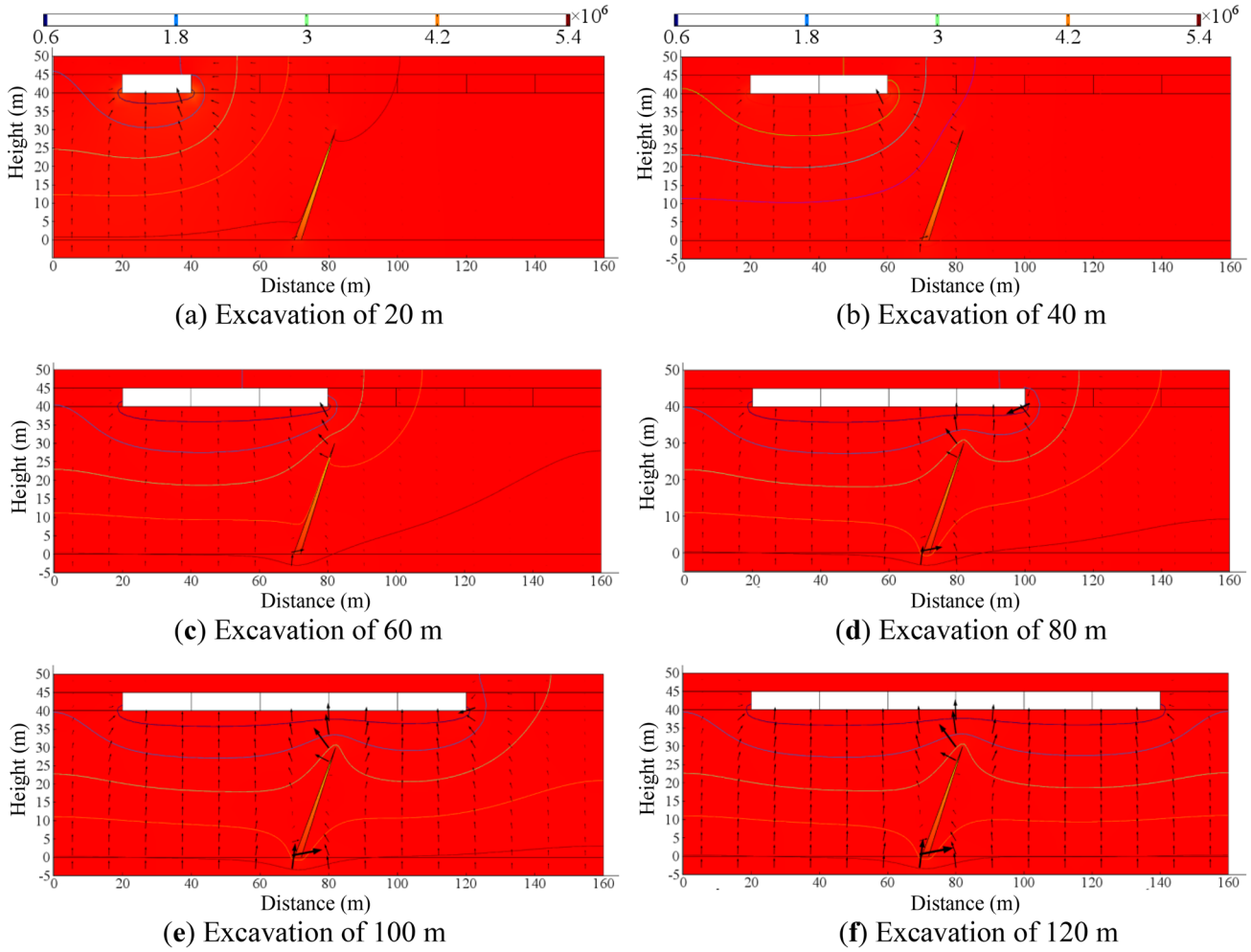

Fig. 6 Seepage pressure field and velocity variation nephogram

At an advancing distance of 60 m, the working face had passed through the buried fault. In the stress unloading area in the lower part of the goaf, the maximum stress changes to 82.9 MPa and the accumulated stress near the fault zone is reduced to 49 MPa (Fig. 5b). The stress inside the fault is far less than in the floor during this time period, which indicates that fissures have been generated in the fault by the concentrated force, destroying the overall structure of the rock.

At 80–100 m, the stress concentrated areas in the floor and the buried fault almost coincide, forming a "stress-transfixion" phenomenon. The faulted rock deforms, creating the water inrush channel.

Seepage Field Variation Analysis

Figure 6 shows the nephogram of the water flow pressure field and flow velocity trend as excavation advanced from 20 to 120 m. The model was simulated using pore water pressure flow, the goaf was designed as a water outlet, and the black arrows express the direction of water flow as well as the magnitude of the flow velocity.

The velocity of water flow inside the fault is much greater than in the floor, which is more consistent with the distribution of the micro-fracture flow (Fig. 6). As the working face advanced, the water flow velocity in the floor gradually increased and the fault area increased significantly. This means that under the combined action of the mining ground pressure and the confined water pressure of the confined aquifer, the original fractures with poor connectivity and weak permeability begin to expand, connect, and penetrate, gradually forming the damaged zone in the floor. The permeability coefficient of the rock mass in the damaged zone was significantly increased, and the water barrier capacity basically lost. At 100 m, the flow velocity in the fault peaked. As the working face continued to advance, the flow velocity remained fairly stable, which indicates that the inrush channel had been formed, causing a water inrush event.

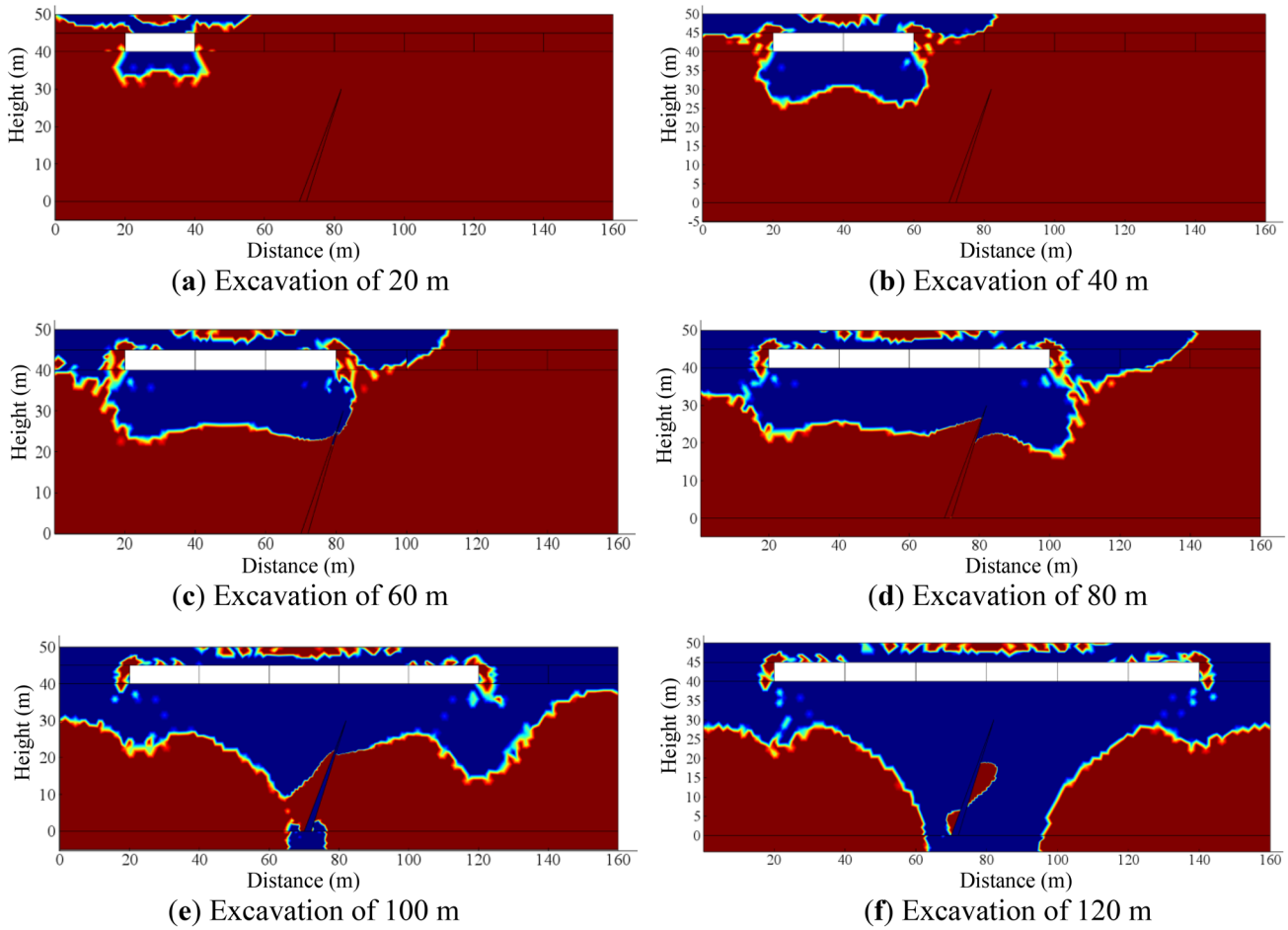

Fig. 7 Floor failure depth nephogram

Analysis of the Floor Failure Depth

Figure 7 shows the simulated nephogram of the floor failure depth. The continuous exploitation of the coal seam has destroyed the initial ground stress equilibrium state of the coal floor, and damage to the floor is obvious. As shown in Fig. 7a–c, the failure depth reaches 5 m and presents a "saddle-shape" at an advance of 20 m. As the working face advanced, the depth and scope of the floor failure area gradually increased. At 60 m, the maximum damage extended about 20 m, at both ends of the goaf and below the open-off cut and working face. Due to the existence of the buried fault, the failure depth changed as mining advanced from 80 to 120 m. At 100 m, the failure area in the middle of the goaf extended downward with a maximum depth of 30 m, and the failure area at the lower end of the buried fault met the damaged zone, creating more water inrush channels. At 120 m, the damage continued to increase, and as the damaged area gradually approached the confined water aquifer, the number of water inrush points increased. The buried fault structure destroyed the integrity of the coal seam floor, and reduced the strength of the water-resisting rock mass and the ability of the aquifuge to resist deformation.

Conclusions

The floor failure and formation of water inrush channel are the result of the coupling of the seepage and stress fields, which were analyzed by studying the anomalous variation of multi field characteristics. The buried fault provided favorable conditions for a floor water inrush when the working face advanced to the fault center.

The stress concentration first formed around the fault structure as the working face advanced. When the working face passed the buried fault, the original stress concentration was released, and fissures were generated in the fault rock, reducing the stress in the fault. With further advancement, a "stress-transfixion" zone appeared, making it easy for a water inrush channel to form. As the working face advanced, the water flow velocity in the floor increased gradually, while the flow velocity in the fault area increased significantly.

Due to the existence of the buried structure, the failure depth of the floor obviously changed as the working face passed the fault. Once the floor failure zone depth reached the fault zone, the water flow velocity in the structure remained relatively stable even as the working face continued to advance, since the water inrush channel had formed. The fissures in the lower part of the fault gradually developed upward to form new water inrush channels, gradually increasing the number of water inrush points.

Acknowledgements This research was financially supported by the National Natural Science Foundation of China (51404146), China Postdoctoral Science Foundation (2015M572067), Postdoctoral Innovation Project of Shandong Province (152799), Key R & D Projects in Shandong Province (2015GSF120016), Qingdao Postdoctoral Applied Research Project (2015203), Young Teachers' Growth Program of Shandong Province, Natural Science Foundation of Shandong Province (ZR2019MEE004) and the Shandong University of Science and Technology (SDUST) Research Fund (2018TDJH102).

References

Bereslavskii EN (2011) Simulation of seepage flows from channels. PMM-J Appl Math Mec 75(4):398–403

Bukowski P (2011) Water hazard assessment in active shafts in upper Silesian coal basin mines. Mine Water Environ 30(4):302–311

Dumpleton S, Robins NS, Walker JA, Merrin PD (2001) Mine water rebound in south Nottinghamshire: risk evaluation using 3-D visualization and predictive modeling. Q J Eng Geol Hydrogeol 34(3):307–319

Feng LQ, Wang WJ, Zhu CQ, Peng WQ (2009) Analysis of fault water-inrush mechanism based on the principle of water-resistant key strata. J Min Saf Eng 26(1):87–90 **(in Chinese)**

Grasemann B, Exner U, Tschegg C (2011) Displacement–length scaling of brittle faults in ductile shear. J Struct Geol 33(11):1650

Hodlur G, Prakash RM, Deshmukh S, Singh V (2002) Role of some salient geo-physical, geochemical, and hydrogeological parameters in the exploration of fresh groundwater in a brackish terrain. Environ Geol 41(7):861–866

Li LP, Zhou ZQ, Li SC, Xue YG, Xu ZH, Shi SS (2015) An attribute synthetic evaluation system for risk assessment of floor water inrush in coal mines. Mine Water Environ 34:288–294

Li WP, Liu Y, Qiao W, Zhao C, Yang DD, Guo QC (2018) An improved vulnerability assessment model for floor water bursting from a confined aquifer based on the water inrush coefficient method. Mine Water Environ 37(1):196–204

Lu Y, Wang L (2015) Numerical simulation of mining-induced fracture evolution and water flow in coal seam floor above a confined aquifer. Comput Geotech 67:157–171

Odintsev VN, Miletenko NA (2015) Water inrush in mines as a consequence of spontaneous hydrofracture. J Min Sci 51(3):423–434

Shao J, Zhou F, Sun W (2019) Evolution model of seepage characteristics in the process of water inrush in faults. Geofluids 2019:1–14

Sun WB, Xue YC (2018) An improved fuzzy comprehensive evaluation system and application for risk assessment of floor water inrush in deep mining. Geotech Geol Eng. https://doi.org/10.1007/s10706-018-0673-x

Sun WB, Du HQ, Zhou F, Shao JL (2019) Experimental study of crack propagation of rock-like specimens containing conjugate fractures. Geomech Eng 17(4):323–331. https://doi.org/10.12989/gae.2019.17.4.323

Wang Y, Yang WF, Li M, Liu X (2012) Risk assessment of floor water inrush in coal mines based on secondary fuzzy comprehensive evaluation. Int J Rock Mech Min 52(6):50–55

Wang T, Wang ZH, Jiang YD, Wang WJ (2014) Experimental study on stress distribution and evolution surrounding rock under the influence of fault slip induced by mining. J China Univ Min Technol 43:588–592 **(in Chinese)**

Wang G, Li W, Wang P, Yang X, Zhang S (2017) Deformation and gas flow characteristics of coal-like materials under triaxial stress conditions. Int J Rock Mech Min 91:72–80

Wu Q, Liu YZ, Wu HX, Zeng YF (2017) Assessment of floor water inrush with vulnerability index method: application in Malan coal mine of Shanxi Province, China. Q J Eng Geol Hydrogeol 50(2):169–178

Xiong ZQ, Wang XL (2014) Similar simulation for breakage law and cracks evolution of working face in coal mining above aquifer. Chin J Undergr Space Eng 10(05):1114–1120 **(in Chinese)**

Yin DW, Chen SJ, Liu XQ, Ma HF (2018a) Effect of joint angle in coal on failure mechanical behavior of roof rock-coal combined body. Q J Eng Geol Hydrogeol 51:202–209

Yin DW, Chen SJ, Liu XQ, Ma HF (2018b) Simulation study on strength and failure characteristics for granite with a set of cross-joints of different lengths. Adv Civ Eng 2018:1–10

Zhang WQ (2004) Study on the mechanism of water-bursting from the floor of mine and its integrated judgment and measure and the software exploitation of forecast system. Ph.D. Dissertation, Shandong University of Science and Technology **(in Chinese)**

Zhang SC, Guo WJ, Li YY, Sun WB, Yin DW (2017) Experimental simulation of fault water inrush channel evolution in a coal mine floor. Mine Water Environ 36:443–451

Zhang SC, Li YY, Shen BT, Sun XZ, Gao LQ (2018) Effective evaluation of pressure relief drilling for reducing rock bursts and its application in underground coal mines. Int J Rock Mech Min 114:7–16. https://doi.org/10.1016/j.ijrmms.2018.12.010

Zhou QL, Herrera J, Hidalgo A (2018) The numerical analysis of fault-induced mine water inrush using the extended finite element method and fracture mechanics. Mine Water Environ 37:185–195